Fast centromeric repeat turnover provides a glimpse into satellite DNA evolution in *Nothobranchius* annual killifishes

Anna Voleníková[1,2], Karolína Lukšíková[1,3], Pablo Mora[2,4], Tomáš Pavlica[1,5], Marie Altmanová[1,6], Jana Štundlová[1,2,5], Šárka Pelikánová[1], Sergey A. Simanovsky[7], Marek Jankásek[1,5], Martin Reichard[8,9,10], Petr Nguyen[1,2¶*], Alexandr Sember[1¶*]

[1] Institute of Animal Physiology and Genetics, Czech Academy of Sciences, Liběchov, Czech Republic
[2] University of South Bohemia, Faculty of Science, České Budějovice, Czech Republic
[3] Department of Genetics and Microbiology, Faculty of Science, Charles University, Prague, Czech Republic
[4] Department of Experimental Biology, Genetics Area, University of Jaén, Jaén, Spain
[5] Department of Zoology, Faculty of Science, Charles University, Prague, Czech Republic
[6] Department of Ecology, Faculty of Science, Charles University, Prague, Czech Republic
[7] Severtsov Institute of Ecology and Evolution, Russian Academy of Sciences, Moscow, Russia
[8] Institute of Vertebrate Biology, Czech Academy of Sciences, Czech Republic
[9] Department of Ecology and Vertebrate Zoology, University of Łódź, Łódź, Poland
[10] Department of Botany and Zoology, Faculty of Science, Masaryk University, Brno, Czech Republic

[*] **Correspondence**: sember@iapg.cas.cz (AS); petr.nguyen@prf.jcu.cz (PN)

¶These authors contributed equally to this work.

ORCID IDs:
A.V.: 0000-0002-9504-8044
P.M.: 0000-0001-7967-3379
M.A.: 0000-0001-7193-8918
J.S.: 0000-0001-7890-1608
S.A.S: 0000-0002-0830-7977
M.J.: 0000-0002-1467-8790
M.R.: 0000-0002-9306-0074
P.N.: 0000-0003-1395-4287
A.S.: 0000-0003-4441-9615

Abstract

Satellite DNA (satDNA) is rapidly evolving class of tandem repeats with some motifs being involved in centromere organization and function. Rapid co-evolution of centromeric satDNA and associated proteins has been mostly attributed to the so-called centromere drive. To identify repeats associated with centromeric regions and test for the role of meiotic drive in their evolution, we investigated satDNA across Southern and Coastal clades of African annual killifishes of the genus *Nothobranchius*. C-banding showed expansion of (peri)centromeric heterochromatin regions in the Southern-clade killifishes. Molecular cytogenetic and bioinformatic analyses further revealed that two previously identified satellites, Nfu-SatA and Nfu-SatB, are associated with centromeres only in one lineage of the Southern clade. Nfu-SatB was, however, detected outside centromeres also in other members of the Coastal clade, which is consistent with the “library” hypothesis of satDNA evolution. We also identified a novel satDNA, Cl-36, associated with (peri)centromeres in *N. foerschi*, *N. guentheri* and *N. rubripinnis* from the Coastal clade. Our findings could be explained by centromere drive shaping karyotype change and centromeric repeat turnover in *Nothobranchius* species with possible reversal of spindle polarity within the Southern clade.

Keywords: centromere drive; chromosome; constitutive heterochromatin; library hypothesis; RepeatExplorer; repetitive sequences; satDNA

1. Introduction

African killifishes from the genus *Nothobranchius* (Peters, 1868) (Aplocheiloidei: Nothobranchiidae) are small freshwater fishes with bigger and more colorful males compared to smaller and dull females (Wildekamp 2004, Berois et al. 2016). The genus is monophyletic and currently comprises over 90 species (Nagy and Watters, 2021, Fricke et al. 2022) partitioned into seven evolutionary lineages (van der Merwe et al. 2021). *Nothobranchius* spp. are adapted to periodic droughts driven by cycles of rainy and dry seasons in south-eastern African savannahs, where they survive in isolated pools, temporarily flooded by rainwater (Blažek et al. 2013, Furness 2016, Cellerino et al. 2016). Having the shortest life cycle among vertebrates, the turquoise killifish *N. furzeri* (Jubb, 1971) became a popular model system for aging research (Cellerino et al. 2016, Hu and Brunet 2018). Besides, the unique biology of killifishes offers many advantages for studies related to developmental biology, population dynamics and evolution (Cellerino et al. 2016, Terzibasi Tozzini and Cellerino 2020). For instance, their mating system and sexual dimorphism make them attractive for studies of reproductive isolation and sexual selection (Berois et al. 2016, Cellerino et al. 2016).

Nothobranchius killifishes became of interest also to genome and sex chromosome research. Studies reported high repetitive DNA content in *Nothobranchius* genomes (Reichwald et al. 2009, 2015, Cui et al. 2019, Štundlová et al. 2022) and wide variation in diploid chromosome numbers (2n = 16–50) and karyotype structures in 73 studied representatives (Krysanov et al. 2016, Krysanov and Demidova 2018, Krysanov et al. 2023). Moreover, a multiple sex chromosome system of the X_1X_2Y type has been cytogenetically identified in six distant *Nothobranchius* spp., which suggests remarkable sex chromosome evolution (Ewulonu et al. 1985, Krysanov et al. 2016, Krysanov and Demidova 2018). Intriguingly, the *N. furzeri* genome sequence revealed an XY sex chromosome pair with polymorphic size of a non-recombining region in different populations (Reichwald et al. 2015, Willemsen et al. 2020). It was hypothesized that the *N. furzeri* Y chromosome polymorphism represents an early stage of sex chromosome evolution (Reichwald et al. 2015). However, physical mapping of various repeats in *N. furzeri* and its sister species *N. kadleci* revealed that repetitive DNA landscape differs considerably between their X and Y chromosomes and these differences extend beyond the non-recombining regions. One particular difference between the X and Y chromosomes was a largely reduced block of constitutive heterochromatin in the centromeric region on Y chromosomes in two out of three examined populations (Štundlová et al. 2022). This region overlapped with hybridization signals of fluorescence *in situ* hybridization (FISH) with two repeats associated with *N. furzeri* centromeres, the Nfu-SatA and Nfu-SatB (Reichwald et al. 2009; Štundlová et al. 2022).

Certain satellite DNAs (satDNA), i.e. tandemly repeated DNA class with rapid molecular evolution (Plohl et al. 2012, Garrido-Ramos 2017, Thakur et al. 2021), can be associated with centromeres (Melters et al. 2013, Hartley and O'Neill 2019, Talbert and Henikoff 2020) and thus are considered to be involved in segregation of chromosomes during cell divisions (Henikoff et al. 2001, McKinley and Cheesman 2016). Yet despite their rather conservative function, centromeric satDNAs turn over very fast (Henikoff et al. 2001, Bracewell et al. 2019, Ávila Robledillo et al. 2020, Nishihara et al. 2021). It has been hypothesized that rapid co-evolution of both centromeric DNA and associated proteins is mainly driven by centromere drive (Henikoff et al. 2001). The hypothesis postulates that homologous chromosomes differ in their capability to bind spindle microtubules and thus can segregate non-randomly exploiting the asymmetric female meiosis, which produces three polar bodies (i.e. the evolutionary dead-ends) and only one egg (Henikoff et al. 2001, Kursel and Malik 2018, Kumon and Lampson 2022). Deleterious segregation errors induce selective pressure, which fuels the evolution of involved proteins and DNA repeats, thus suppressing the drive (Henikoff et al. 2001, Kumon and Lampson 2022).

Hence, it was hypothesized that the reduction in centromeric clusters of the Nfu-SatA and Nfu-SatB repeats on Y chromosomes observed in *N. furzeri* reflects relaxed selection imposed by centromere drive (Štundlová et al. 2022), as the Y chromosome never passes through female meiosis (cf. Yoshida and Kitano 2012, Pokorná et al. 2014). Unfortunately, nothing is known about killifish centromeric organization outside *N. furzeri* and *N. kadleci* (Reichwald et al. 2009, 2015; Štundlová et al. 2022) and little is known about the centromere organization in teleost fishes in general. Rather than identifying sequences which bind centromeric proteins (Cech and Peichel 2016, Ichikawa et al. 2017), the available studies have focused mainly on sequences associated with centromeres, detected either by molecular or bioinformatic methods and physically mapped by means of *in situ* hybridization (Ferreira et al. 2010, Suntronpong et al. 2020, Stornioli et al. 2021, Goes et al. 2022, 2023, Kretschmer et al. 2022). More recently, these sequences have been inferred directly from long read sequencing data (Ichikawa et al. 2017, Conte et al. 2019, Varadharajan et al 2019, Tao et al. 2021). These are typically satellite sequences presumably containing conserved motifs such as the CENP-B box needed for chromosome stability and cell division (Suntronpong et al. 2016; Gamba and Fachinetti 2020). Centromeric tandem repeats seem to be homogenized at higher rates in teleost fishes compared to other vertebrates (Suntronpong et al. 2020) and their evolutionary dynamics seems to reflect centromeric position with those of acrocentrics being more conserved (Ichikawa et al. 2017).

In the present study, we analyzed repetitive sequences across the representatives of *Nothobrachnius* genus by means of RepeatExplorer2 bioinformatic pipeline (Novák et al. 2020) to identify repeats associated with centromeric regions and to look for evidence of centromere

drive. Our results suggest that Nfu-SatA and Nfu-SatB are associated with centromeres only in one lineage of the Southern clade, although Nfu-SatB can be detected also in representatives of the Coastal clade, in agreement with the "library" hypothesis (i.e. the existence of shared collection of satDNA repeats among related species, with varied degree of their amplification and contraction; Fry and Salser 1977, Ruiz-Ruano et al. 2016). We also identified novel repeat associated with centromeres in the Coastal-clade species. Based on the presence of larger (peri)centromeric heterochromatin blocks observed in the Southern-clade species but not in other studied representatives, we discuss a possible reversal of spindle orientation in the common ancestor of this clade.

2. Materials and Methods

2.1 Fish sampling

We analyzed individuals of 14 species representing the Southern and Coastal clade (seven and five species, respectively) of the genus *Nothobranchius*, with *N. ocellatus* and *Fundulosoma thierryi* as their outgroups. The studied individuals from *N. orthonotus*, *N. kuhntae*, *N. pienaari*, *N. rachovii*, *N. eggersi* and *N. rubripinnis* were sampled from laboratory populations recently derived from wild-caught individuals and were previously identified based on morphology and the phylogenetic analysis of mitochondrial and nuclear DNA markers (for details, see Bartáková et al. 2015; Blažek et al. 2017; Reichard et al. 2022). The remaining species were obtained from specialists and experienced hobby breeders who keep strictly population-specific lineages derived from original imports. In this case, the species identity was confirmed on the basis of key morphological characters (Wildekamp 1996, 2004; Watters et al. 2008, 2020; Nagy 2018). The detailed information is provided in Table 1.

Table 1. List of *Nothobranchius* killifish species used in this study along with their sample sizes (N) and origin.

Clade	Species	Code	N*	Source / locality
outgroup	*Fundulosoma thierryi* Ahl, 1924	FTH	1♂, 3♀	aquarium strain
Southern clade	*Nothobranchius furzeri* Jubb, 1971	NFU	1♂, 1♀	Chefu, MZ
	N. kadleci Reichard, 2010	NKA	1♂, 1♀	Gorongosa, MZ
	N. orthonotus (Peters, 1844)	NOR	3♂, 3♀	Limpopo, MZ
	N. kuhntae (Ahl, 1926)	NKU	4♂, 3♀	Pungwe, MZ
	N. pienaari Shidlovskyi, Watters & Wildekamp, 2010	NPI	2♂, 3♀	Limpopo, MZ
	N. krysanovi Shidlovskyi, Watters & Wildekamp, 2010	NKR	2♂, 2♀	Quelimane, MZ
	N. rachovii Ahl, 1926	NRA	2♂, 2♀	Beira Airport, MZ
Ocellatus clade	*N. ocellatus* (Seegers, 1985)	NOC	1♂, 1♀	Nyamwage, TZ
Coastal clade	*N. eggersi* Seegers, 1982	NEG	2♂, 1♀	Bagamoyo, TZ
	N. foerschi Wildekamp & Berkenkamp, 1979	NFO	2♂	Soga, TZ
	N. guentheri (Pfeffer, 1983)	NGU	4♂, 3♀	Zanzibar, TZ
	N. cardinalis Watters, Cooper & Wildekamp, 2008	NCA	1♂	Matandu, TZ
	N. rubripinnis Seegers, 1986	NRU	2♂, 2♀	Kitonga, TZ

* number and sex of individuals used for each method is specified in Supplementary Table 1

2.2 Chromosomal preparations

Mitotic chromosome spreads were obtained either i) from regenerating caudal fin tissue (Völker and Ráb 2015) with modification described in Sember et al. (2015) and a fin regeneration time ranging from one to two weeks, or ii) by a direct preparation from the cephalic kidney following Ráb and Roth (1988) and Kligerman and Bloom (1977), with in the latter protocol being modified according to Krysanov and Demidova (2018). In the kidney-derived preparations, the chromosomal spreading quality was enhanced using a dropping technique by Bertollo et al. (2015). Preparations were inspected with phase-contrast optics and those of sufficient quality were dehydrated in an ethanol series (70%, 80%, and 96%, 2 min each) and stored at -20 °C until use.

2.3 Constitutive heterochromatin staining

Analysis of constitutive heterochromatin distribution was done by C-banding (Haaf and Schmid 1984), using 4′,6-diamidino-2-phenolindole (DAPI) (1.5 µg/mL in anti-fade; Cambio, Cambridge, UK) counterstaining. Fluorescent staining with the GC-specific fluorochrome Chromomycin A_3 (CMA_3) and the AT-specific fluorochrome DAPI (both Sigma-Aldrich, St. Louis, MO, USA) was performed according to Mayr et al. (1985) and Sola et al. (1992).

2.4 Whole-genome sequencing data

Genomic DNA was sequenced *de novo* in *Nothobranchius guentheri*, *N. kadleci*, *N. orthonotus*, *N. rachovii* and *N. rubripinnis*. First, high molecular weight genomic DNA (HMW gDNA) was extracted from three females of each species using a MagAttract HMW DNA Kit (Qiagen, Hilden, Germany), following the provided protocol. Next, Illumina paired-end libraries with 450 bp insert size were prepared from the isolated HMW gDNA and sequenced on the NovaSeq 6000 platform at Novogene (HK) Co., Ltd. (Hong Kong, China), yielding, at least, 5 Gb (ca 3.3× coverage of *Nothobranchius furzeri* genome; 1C = 1.54 Gb, Reichwald et al. 2009). Resulting data were deposited into the Sequence Read Archive (SRA) under accession numbers XXX – XXX. In *N. furzeri* and *N. kadleci*, sequencing data from three female specimen were obtained from the SRA (accession numbers ERR583470, ERR58471, SRR1261480; Reichwald et al. 2015, and XXX, XXX, XXX; Štundlová et al. 2022, respectively).

2.5 Analysis of repetitive DNA

The satellitome was characterized using RepeatExplorer2 (Novák et al. 2020). Prior to the analysis, the quality of raw Illumina reads was checked using FastQC (version 0.11.5; Andrews 2010). Low quality reads and adapter sequences were removed using cutadapt (version 1.15; Martin 2011) with settings for two-color chemistry: '--nextseq-trim=20 -u -50 -U -50 -m 100 -a AATGATACGGCGACCACCGAGATCTACACTCTTTCCCTACACGACGCTCTTCCGATCT -

A GATCGGAAGAGCACACGTCTGAACTCCAGTCACNNNNNNATCTCGTATGCCGTCTTCTG CTTG'. For comparative analysis, 1,600,000 reads (ca 0.1× genome coverage of *N. furzeri*) were pseudorandomly subsampled from each biological replica of each species and resulting subsets were concatenated and analyzed together. The RepeatExplorer2 pipeline was run on the Galaxy server (The Galaxy Community 2022) with Metazoa version 3.0 protein domain database and automatic filtering of abundant repeats. In addition, the repeats were studied in each species independently, using a set of 7,125,000 reads (ca 0.5× coverage) and equivalent RepeatExplorer2 parameters. Calculation of G+C content and reciprocal BLAST were performed in GeneiousPrime (version 2020.1.2; https://www.geneious.com). To target potential centromeric repeats, the results of the single-species analysis were confined to high confidence satellites with estimated abundance in the genome at least 0.15% and monomer length <1kb only.

2.6 Fluorescent in situ hybridization (FISH)

2.6.1. Preparation of FISH probes

We previously characterized Nfu-SatA and Nfu-SatB as the most abundant satellite DNA motifs in *N. furzeri* and *N. kadleci* (Štundlová et al. 2022). For FISH, the probe covering the whole monomer length 77 bp of Nfu-SatA was generated by 5' labeling with Cy3 during synthesis (Generi Biotech, Hradec Králové, Czech Republic). In the same way, the probes for the Cl-36, Cl-127, Cl-260 and Cl-294, characterized for the first time in the present study (see below), have been prepared. In the case of Nfu-SatB (348-bp-long monomer), the clones with inserts containing three adjacent tandemly arrayed Nfu-SatB monomers which were prepared and verified in the previous study (Štundlová et al. 2022) were used for the FISH probe preparation. The entire plasmids were labeled by nick translation using a Cy3 NT Labeling Kit (Jena Bioscience, Jena, Germany). For the final probe mixture preparation, 250–500 ng of labeled plasmid and 12.5–25 µg of sonicated salmon sperm DNA (Sigma-Aldrich) were applied per slide. The final hybridization mixtures for each slide (15 µL) were prepared according to Sember et al. (2015).

2.6.2. Standard FISH analysis

Single-color FISH experiments with Nfu-SatB probe were carried out following Sember et al. (2015) (slide pre-treatment, probe/chromosomes denaturation and hybridization conditions) and Yano et al. (2017) (post-hybridization washing), with modifications described in Štundlová et al. (2022). Briefly, following standard pre-treatment steps, chromosomes were denatured in 75% formamide in 2× SSC (pH 7.0) (Sigma-Aldrich) at 72 °C for 3 min. The hybridization

mixture was denatured at 86 °C for 6 min. The hybridization took place overnight (17–24h) at 37 °C in a moist chamber. Subsequently, non-specific hybridization was removed twice in 1× SSC (pH 7.0) (65 °C, 5 min each) and once in 4× SSC in 0.01% Tween 20 (42 °C, 5 min), followed by washing in 1× PBS (1 min). Slides were dehydrated in an ethanol series (70%, 80%, and 96%, 2 min each) and then mounted in anti-fade containing 1.5 µg/mL DAPI (Cambio, Cambridge, UK).

2.6.3. Non-denaturing FISH (ND-FISH)

Remaining five satDNA probes (Nfu-SatA, Cl-36, Cl-127, Cl-260 and Cl-294; more details provided in section 3.2) were mapped using ND-FISH according to Cuadrado and Jouve (2010) with some modifications. Briefly, a total of 30 µL of hybridization mixture containing 2 pmol/µL of oligonucleotides (labeled at 5' end with Cy3) in 2× SSC were used per slide. Then the mixture was denatured at 80 ºC for 5 min and immediately placed on ice. After that, the denatured hybridization mixture was transferred into the slides with neither pre-treatment steps nor chromosome denaturation. After two hours of hybridization at room temperature (RT), the slides were washed with 4× SSC 0.2% Tween-20 at RT and shaking for 10 min, followed by 5 min washing in 4× SSC 0.1% Tween-20 also at RT and shaking. Chromosome preparations were then passed through ethanol series (70%, 80% and 96%, 3 min each) and then air dried. Chromosomes were counterstained with 20 µL of DABCO anti-fade (1,4-diazabicyclo(2.2.2)-octane containing 0.2 µg/mL DAPI (both Sigma-Aldrich) or in anti-fade containing 1.5 µg/mL DAPI Cambio, Cambridge, UK).

2.7. Microscopic analyses and image processing

Images from all cytogenetic methods were captured using a BX53 Olympus microscope equipped with an appropriate fluorescence filter set and coupled with a black and white CCD camera (DP30W Olympus). Images were acquired for each fluorescent dye separately using DP Manager imaging software (Olympus), which was further used also to superimpose the digital images with the pseudocolors (red for CMA_3 and green for DAPI in case of fluorescence staining; blue for DAPI and red for Cy3 in case of FISH). Composite images were then optimized and arranged using Adobe Photoshop, version CS6.

At least 20 chromosome spreads per individual and method were analyzed. Chromosomes were classified according to Levan et al. (1964), but modified as m – metacentric, sm – submetacentric, st – subtelocentric, and a – acrocentric, where st and a chromosomes were scored together into st-a category.

3. Results

3.1 Cytogenetics

Basic karyotype characteristics

Individuals from all studied species displayed mostly the same 2n and highly similar proportion of chromosome categories as previously reported (Reichwald et al. 2009, 2015; Krysanov and Demidova 2018). The only exception was *N. ocellatus*, where we recorded 2n = 32 with the karyotype being composed exclusively of monoarmed (st-a) chromosomes, in contrast to previously reported 2n = 30 with one chromosome pair being large metacentric (Krysanov and Demidova 2018). The individuals studied by Krysanov and Demidova (2018) were later found to be members of a newly described closely related species *N. matanduensis* (Watters et al. 2020) (S. Simanovsky, pers. commun.). Finally, in line with the previous reports (Ewulonu et al. 1985, Krysanov and Demidova 2018), *Fundulosoma thierryi* and *N. guentheri* possessed male heterogametic $X_1X_1X_2X_2/X_1X_2Y$ multiple sex chromosome system manifested by different chromosome counts between males and females (males had one chromosome less) and particularly in *N. guentheri* the male-limited neo-Y chromosome was discernible as the only large sm/st element in the complement.

Distribution and composition of constitutive heterochromatin

Amount of constitutive heterochromatin varied among the studied *Nothobranchius* spp. (Supplementary Fig. 1). The outgroup taxon *F. thierryi* together with *Nothobranchius* species from the Southern clade possessed generally more heterochromatin segments than *N. ocellatus* and species from the Coastal clade where the narrow C-bands were confined mostly to the (peri)centromeric regions of overwhelming majority (*N. cardinalis, N. ocellatus*), two-thirds (*N. rubripinnis*), about half (*N. eggersi*, *N. guentheri*) or several chromosomes (*N. foerschi*) of the complement. Within the chromosome complements of *N. cardinalis*, *N. guentheri* and *N. rubripinnis*, the largest metacentric chromosome pair either lacked or had unremarkable/ notably smaller C-bands compared to the remainder of the chromosome set (Supplementary Fig. 1J–M). In *N. foerschi*, the largest metacentric chromosome pair possessed a distinct (peri)centromeric C-band, while the second largest metacentric pair displayed only tiny heterochromatin block (Supplementary Fig. 1I). By contrast, majority of large biarmed chromosomes in species of the Southern clade possessed large heterochromatin segments (see below). In addition to (peri)centromeric bands, heterochromatin accumulations were present on the short arms of several chromosomes in *N. eggersi*. In males of *N. guentheri*, neo-Y sex chromosome bore an apparent C-banded region on its long arms Supplementary Fig. 1J, arrowhead). The other species with known X_1X_2Y multiple sex chromosome system (*F. thierryi*) did not show any exceptional C-banding pattern

315 on these sex chromosomes. Four st-a chromosomes in *F. thierryi* displayed remarkable
316 heterochromatin blocks covering their short arms. In the Southern clade, *N. orthonotus* and *N.*
317 *kuhntae* featured the highest amount and diversity of heterochromatin blocks which were
318 distributed on multiple regions across the chromosome complement. This observation is
319 consistent with large (peri)centromeric regions found previously in closely related *N. furzeri*
320 and *N. kadleci* (Štundlová et al. 2022; see Supplementary Fig. 2A, B for comparison). On the
321 other hand, chromosomes of *N. pienaari*, *N. krysanovi* and *N. rachovii* bore almost exclusively
322 (peri)centromeric bands of variable lengths, some of them being remarkably large
323 (Supplementary Fig. 1D–F). In the species with almost exclusively biarmed (metacentric or
324 submetacentric) chromosomes and low 2n, namely *N. krysanovi* and *N. rachovii*, some
325 (peri)centromeres were arranged as two large adjacent blocks. *N. krysanovi* also displayed
326 additional interstitial heterochromatin blocks on several chromosomes. In *N. rachovii* only two
327 large submetacentric chromosomes possessed very tiny interstitial bands in addition to
328 (peri)centromeric ones.
329 Fluorescent staining revealed, besides few predominantly $DAPI^+$ (AT-rich) bands (e.g.,
330 in *F. thierryi*, *N. orthonotus*), variable amount and distribution of CMA_3^+ (GC-rich) regions. Five
331 species (*F. thierryi*, *N. pienaari*, *N. krysanovi* and *N. foerschi*) displayed just one pair of clear
332 terminal or interstitial signals, highly likely overlapping with major ribosomal DNA (rDNA)
333 cluster (cf. Sember et al. 2015 and references therein). Similar signals were revealed also on
334 the neo-Y and at least one X chromosome of *N. guentheri* (Supplementary Fig. 3J). Several
335 *N. guentheri* chromosomes also featured additional tiny centromeric signals on at least four
336 chromosomes (Supplementary Fig. 3J, K). In *N. rachovii*, terminal CMA_3^+ signals were
337 observed on the short arms of the smallest acrocentric chromosome pair, and at least four
338 large metacentrics/submetacentrics had a tiny centromeric signal (Supplementary Fig. 3F). *N.*
339 *ocellatus* and *N. eggersi* bore up to seven and up to four signals, respectively. *N. cardinalis*
340 and *N. rubripinnis* shared the CMA_3 pattern in the way that (peri)centromeres of all
341 chromosomes were GC-rich except for the one pair of large metacentric chromosomes. Finally,
342 almost all chromosome pairs in *N. orthonotus* and *N. kuhntae* had GC-rich (peri)centromeres,
343 similarly to patterns found in *N. furzeri* and *N. kadleci* (Štundlová et al. 2022; Supplementary
344 Fig. 2C, D).
345
346 **3.2 Identification of candidate repeats**
347 The comparative analysis of tandem repeats in representatives of the Southern (*N. furzeri*, *N.*
348 *kadleci*, *N. orthonotus*, *N. rachovii*) and Coastal (*N. guentheri*, *N. rubripinnis*) clades revealed
349 in total 21 high confidence satellites with various abundances (Table 2). The two most
350 abundant tandem repeats, namely Cl-11 and Cl-26, were the previously studied putative
351 centromeric repeats Nfur-SatB and Nfur-SatA, respectively. Besides *N. furzeri* and *N. kadleci*,

these clusters were also enriched in *N. orthonotus*, however, limited or completely missing in *N. rachovii*, *N. guentherii* and *N. rubripinnis*, suggesting existence of different motifs in centromeres of these species. Interestingly, satellites Cl-36 and Cl-294 showed the opposite pattern, as they were present in *N. rubripinnis* and *N. guentherii* but missing in the rest of the surveyed taxa. Single-species analysis with more stringent criteria (estimated abundance in the genome at least 0.15%, monomer length <1kb) confirmed these results. Besides already identified markers, one more abundant satDNA (Cl-127) was identified to be shared by multiple species and was therefore included in further analysis, as well as Cl-260, which showed a high number of similarity hits with the above mentioned Nfu-SatA (Cl-26) (Table 3).

Intriguingly, we found a putative CENP-B box in Nfu-SatB repeat. More specifically, a 12bp-long motif (CTTCGTNNNANA) which is highly similar to 17bp-long human core CENP-B recognition sequence (NTTCGNNNNANNCGGGN) (cf. Suntronpong et al. 2016). This finding along with the length of Nfu-SatB motif (348 bp; i.e. approx. twice the length of the nucleosome unit) suggests a possible role of Nfu-SatB in centromere function (Talbert and Henikoff 2020). In contrast to these findings, Nfu-SatA and Cl-36 satellites lacked the mentioned features.

Table 2. High confidence satellites identified by comparative analysis with RepeatExplorer2. Markers selected for physical mapping are indicated in bold.

Satellite	Monomer (bp)	GC (%)	Avg reads per replica						Notes
			NFU	NKA	NOR	NRA	NGU	NRU	
Cl-11	**348**	**41.1**	**2,933**	**1,508**	**643**	**50**	**23**	**9**	**Previously identified Nfu-SatB***
Cl-26	**77**	**63.6**	**560**	**2,533**	**369**	**0**	**2**	**0**	**Previously identified Nfu-SatA***
Cl-28	169	36.1	466	164	4,700	34	18	50	
Cl-36	**48**	**45.8**	**0**	**0**	**0**	**0**	**195**	**2,107**	**Specific for Coastal clade**
Cl-97	93	60.2	398	1,240	262	42	521	233	
Cl-127	**39**	**20.5**	**1,160**	**836**	**19**	**21**	**14**	**28**	**High abundance in multiple species**
Cl-147	349	60.2	62	313	119	108	33	996	
Cl-156	49	65.3	1,261	217	30	0	0	0	
Cl-187	84	31	763	214	86	207	178	68	
Cl-238	24	58.3	556	27	3	2	13	7	
Cl-260	**76**	**57.9**	**0**	**512**	**2**	**0**	**0**	**0**	**Similarity hits with Nfu-SatA (Cl-26)**
Cl-274	662	46.8	1	0	10	163	266	2	
Cl-278	21	19	304	20	56	14	17	18	
Cl-286	20	45	0	0	356	0	1	4	
Cl-294	**63**	**31.7**	**0**	**0**	**0**	**0**	**193**	**137**	**Specific for Coastal clade**
Cl-297	691	42.1	87	46	67	45	35	37	
Cl-310	976	40.1	47	31	40	48	41	61	
Cl-327	980	37.3	49	42	29	37	29	41	

Cl-335	625	43.3	0	0	208	0	0	0	
Cl-342	580	36.9	39	27	29	20	39	39	
Cl-367	490	44.3	27	15	16	29	33	44	

*Reichwald et al. 2009; Štundlová et al. 2022

Table 3. Species-specific analysis of the most abundant satellites (abundance >0.15% of the genome, monomer length < 1kb). Markers selected for physical mapping are indicated in bold.

Species	Cluster	Satellite ID (from comparative analysis)	Estimated genome proportion (%)	Notes
N. furzeri	**NFU-1**	**Cl-11**	**16**	**Previously identified Nfu-SatB***
	NFU-12	**Cl-26**	**3.5**	**Previously identified Nfu-SatA***
	NFU-7	**Cl-127**	**0.48**	
	NFU-8	Cl-156	0.47	
	NFU-29	Cl-238	0.27	
N. kadleci	**NKA-1**	**Cl-26**	**9.6**	**Previously identified Nfu-SatA***
	NKA-2	**Cl-11**	**7.5**	**Previously identified Nfu-SatB***
	NKA-15	Cl-97	0.48	
	NKA-34	**Cl-127**	**0.34**	
N. orthonotus	**NKA-59**	**Cl-11**	**2.3**	**Previously identified Nfu-SatB***
	NKA-1	Cl-28	2.2	
	NKA-24	**Cl-26**	**0.41**	**Previously identified Nfu-SatA***
N. rachovii	No satellites fitting the criteria were identified			
N. guentheri	**NGU-94**	**Cl-36**	**0.18**	
N. rubripinnis	**NRU-1**	**Cl-36**	**2**	
	NRU-23	Cl-147	0.37	

*Reichwald et al. 2009; Štundlová et al. 2022

3.3 Physical mapping of satDNA

FISH with Nfu-SatA (Cl-26) probe revealed detectable clusters only in *N. orthonotus* and *N. kuhntae* (Supplementary Fig. 4B–D). All signals were restricted to (peri)centromeric regions of almost all chromosomes, corroborating patterns found in *N. furzeri* and *N. kadleci* (Štundlová et al. 2022; Supplementary Fig. 2E, F). Whilst all *N. kuhntae* individuals shared the same pattern (i.e., all but one chromosome pair carrying the signal; Supplementary Fig. 4D), individuals of *N. orthonotus* displayed site-number variability, with the number of chromosomes lacking the signal being either four (1 male), five (1 male, 1 female), or six (two males, one female) chromosomes (Supplementary Fig. 4B–C).

Detectable clusters of Nfu-SatB (Cl-11) were found in (peri)centromeric regions of all chromosomes in *N. orthonotus*, *N. kuhntae* (i.e. the same pattern as in *N. furzeri* and *N. kadleci*; Štundlová et al. 2022 and Supplementary Fig. 2G, H), and in (peri)centromeric or terminal regions of about one-third of the chromosome complement in *N. pienaari*

(Supplementary Fig. 5B–D). Besides these species of Southern clade, we also found clear hybridization patterns in three species of Coastal clade. Individuals of *N. eggersi* showed four signals placed terminally on short arms of st-a chromosomes. *N. foerschi* and *N. cardinalis* each carried one pair of st-a chromosomes with (peri)centromeric signals. The pair was small-sized in *N. cardinalis* and among the largest in *N. foerschi*. The Nfu-SatB loci in *N. foerschi* coincided with CMA_3^+ sites (compare Supplementary Figs 3I and 5I).

Satellite repeat Cl-36 was detected only in three species of Coastal clade: *N. rubripinnis* (from which it was isolated), *N. foerschi* and *N. guentheri* (Supplementary Fig. 6K, L, N). The repeat clusters were located exclusively in the (peri)centromeric regions but none of the mentioned species possessed them in all chromosomes. Studied *N. foerschi* and *N. guentheri* males displayed 12 and 16 signals, respectively (Supplementary Fig. 6K, L). In *N. rubripinnis*, 22 out of 36 chromosomes bore the signal (Supplementary Fig. 6N).

The second satellite limited to *N. rubripinnis* and *N. guentheri* (Cl-294) was hybridized in both these species, however, signals were detected only on the long arms of four chromosomes in *N. rubripinnis* (Supplementary Fig. 7A, B). The lack of signal in *N. guentheri* could be explained either by its abundance being below the FISH detection threshold, or by different organization of this repeat in the genome.

Cl-127, shared by *N. furzeri* and *N. kadleci,* was present in both sexes of these species, but no positive FISH signals were observed in *N. orthonotus* (Supplementary Fig. 7C–E). In both species, signals were localized in the long arm of two pairs of chromosomes in both males and females.

The last hybridized marker was Cl-260, bearing similarity hits with Nfu-SatA (Cl-26). Positive signals from this satDNA were observed in all centromeres in both sexes of *N. furzeri* and *N. kadleci*. The only difference in the signal pattern between these two species was related to additional prominent signals located terminally on the short arms of two (*N. furzeri*) and four (*N. kadleci*) chromosomes, respectively (Supplementary Fig. 7F, G).

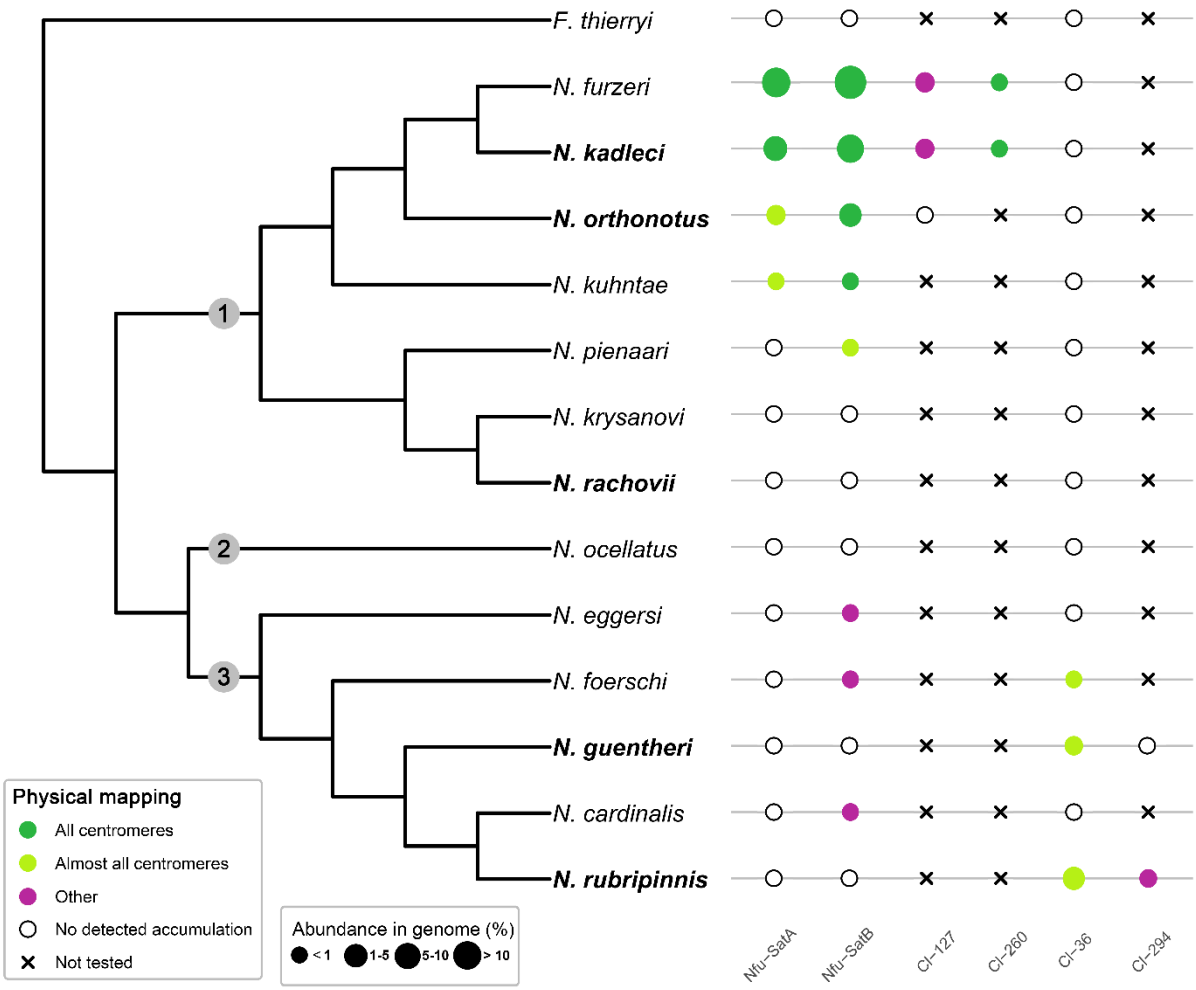

Figure 1: Phylogenetic relationships and patterns of selected repetitive DNA in inspected *Nothobranchius* species. Simplified phylogenetic tree is based on van der Merwe et al. (2021). Colored circles represent positive FISH signals in different chromosomal locations. The size of the circles reflects the abundance in the genome for respective satDNA. Abundance in the genome (%) is set as ranges. Lack of positive signals after FISH is demarcated by empty circles. Black crosses indicate that a given satDNA was not physically mapped in the particular species. Note that abundance in the genome might not perfectly correlate with chromosomal distribution revealed by physical mapping, because some portion of respective tandem repeats may be present in low-copy clusters undetectable by FISH. Species which were subject to RepeatExplorer2 analysis are shown in bold. Numbers in grey circles in the phylogenetic tree denote distinct *Nothobranchius* clades: 1) Southern Clade; 2) Ocellatus Clade; 3) Coastal Clade

4. Discussion

In the present study, we performed a comparative cytogenetic and bioinformatic analyses of satellite DNA across the species of Southern and Coastal clade of the killifish genus *Nothobranchius* to reveal dynamics of repeats associated with centromeres and possible role of meiotic drive in their turnover.

Our results showed that the outgroup *F. thierryi* as well as *Nothobranchius* spp. of the Southern clade, namely *N. orthonotus*, *N. kuhntae*, *N. pienaari*, and *N. rachovii*, have in general more C-banded heterochromatin than representatives of the Coastal clade and their outgroup *N. ocellatus.* The presence of extended C-banded (peri)centromeric heterochromatin regions in large metacentric chromosomes of *N. pienaari*, *N. krysanovi* and *N. rachovii* (Supplementary Fig. 1D–F) is consistent with our previous findings in the remaining Southern-clade species, *N.* furzeri and *N. kadleci* (Štundlová et al. 2022 and Supplementary Fig. 2A, B) where we reported large amounts of (peri)centromeric heterochromatin in almost all chromosomes of the complement. By contrast, our present study shows only narrow C-bands in (peri)centromeric regions of majority of chromosomes in *N. cardinalis*, *N. ocellatus,* and *N. rubripinnis* (Supplementary Fig. 1G, L, M), and in about half-to-several chromosomes in *N. eggersi*, *N. foerschi* and *N. guentheri* (Supplementary Fig. 1H–J). Interestingly, with the sole exception of one chromosome pair in *N. foerschi*, large metacentric chromosomes originating from fusions either lacked or had unremarkable or notably smaller C-bands than other chromosomes in Coastal-clade species (*N. cardinalis*, *N. foerschi*, *N. guentheri* and *N. rubripinnis*). These findings indicate differences in mechanisms underpinning direction of karyotype change between Southern-clade and Coastal-clade killifishes.

To characterize the satDNA evolution, we sequenced and analyzed short reads of *N. guentheri*, *N. kadleci*, *N. orthonotus*, *N. rachovii* and *N. rubripinnis* together with data available for the model species *N. furzeri*. In total, the RepeatExplorer2 comparative analysis revealed 21 satellite sequences. We have analyzed the distribution of the most abundant satellites in all species (Nfu-SatA, Nfu-SatB, Cl-36 and Cl-127) and two additional markers (Cl-260 sharing similary with Nfu-SatA and Cl-294 specific for the Coastal clade) across both clades and the outgroups by FISH.

Štundlová et al. (2022) reported two satDNA motifs, Nfu-SatA and Nfu-SatB, previously identified in the *N. furzeri* strains (Reichwald et al. 2009, 2015) to be the most abundant repeat types in both the *N. furzeri* and *N. kadleci* genomes. Both Nfu-SatA and Nfu-SatB were mapped to (peri)centromeric constitutive heterochromatin blocks of varying sizes in these two sister species (see also Supplementary Fig. 2 C–F). Our results suggest that Nfu-SatA is restricted only to the *N. furzeri* lineage as it is present, although in lower abundance,

also in (peri)centromeric regions of almost all chromosomes in *N. orthonotus* and *N. kuhntae* (Supplementary Fig. 4B–D). Lastly, the satellite Cl-260, was detected in the (peri)centromeric regions of all chromosomes in *N. furzeri* and *N. kadleci* only (Supplementary Fig. 7F, G). While Cl-260 is highly likely a new sequence variant of Nfu-SatA, specific for *N. kadleci* genome only (Table 2), its high sequence similarity with Nfu-SatA was apparently responsible for observing a positive hybridization also in (peri)centromeres of *N. furzeri*.

Nfu-SatB was also detected in (peri)centromeric regions of all chromosomes in *N. orthonotus* and *N. kuhntae* (Supplementary Fig. 5B, C). However, it was further present in detectable amounts also in *N. pienaari* as well as *N. eggersi*, *N. foerschi*, and *N. cardinalis* of the Coastal clade (Supplementary Fig. 5D, H, I, K). The Nfu-SatB signals were located terminally on the short arms of two chromosome pairs in *N. eggersi*, while they resided in (peri)centromeric regions of about one-third of the complement in *N. pienaari* and one chromosome pair of each *N. foerschi* and *N. cardinalis*. Observed pattern is consistent with the “library” hypothesis (Fry and Salser 1977, Ruiz-Ruano et al. 2016) as Nfu-SatB seems to be shared across *Nothobranchius* spp. but it got amplified and associated with centromeres in the *N. furzeri* lineage of the Southern clade.

While Nfu-SatA and Nfu-SatB were found restricted to Southern clade species, satellites Cl-36 and Cl-294 mirrored this pattern as they were detected in the Coastal clade only. The Cl-294 was localized on the long arms of only four chromosomes in *N. rubripinnis* and could not have been detected by FISH on chromosomes of *N. guentheri* (Supplementary Fig. 7A, B). However, Cl-36 was successfully mapped in three representatives of the Coastal clade (Supplementary Fig. 6K, L, N). The hybridization signals were detected exclusively in the (peri)centromeric regions of majority but not all chromosomes in *N. rubripinnis, N. foerschi*, and *N. guentheri.* Corroborating the C- and fluorescent-banding patterns, Cl-36 clusters were absent in (peri)centromeres of some large metacentric chromosomes (Supplementary Fig. 6K, N). This observation is analogous to previously reported satellite-free centromeres, which emerged upon Robertsonian fusions in zebras (Cappelletti et al. 2022).

Interestingly, none of the above tested markers was detected in centromeres of *N. rachovii* (Supplementary Figs. 3F, 4F, 5F, 6H) and the RepeatExplorer2 analysis failed to identify any potentially centromeric satellites in this species (Tab. 2, Tab. 3). Since blocks of (peri)centromeric heterochromatin (Supplementary Fig. 1F), visible on most *N. rachovii* chromosomes, suggest the presence of tandem arrays rather than satellite-free centromeres, a possible explanation might be that microsatellites are the involved sequences in this case. Centromeric localization of short repeat motifs has been described before in various organisms (e.g. Kim et al. 2002, Chang et al. 2008) and their presence could escape RepeatExplorer2 analysis as this tool is known to omit low complexity sequences (Novák et al. 2020).

Differences between X- and Y-linked (peri)centromeric heterochromatin comprising Nfu-SatA and Nfu-SatB were reported in *N. furzeri* and *N. kadleci*, with the Y-linked heterochromatin being considerably reduced (Štundlová et al. 2022). It was hypothesized that this is due to absence of centromere drive on the Y chromosome as it is never transmitted via female meiosis (cf. Yoshida and Kitano 2012; Pokorná et al. 2014). Identification of putative centromeric repeat in the Coastal clade potentially presents an opportunity to test this hypothesis as *N. guentheri* has a multiple sex chromosome system of the X_1X_2Y type, in which neo-Y and one of the X chromosomes can be identified by CMA_3 staining (Supplementary Fig. 3J). However, FISH with Nru-Sat1 failed to detect any satDNA clusters on both the neo-Y and the CMA_3-positive X chromosome.

It was hypothesized that karyotype evolution is driven by meiotic drive in many animal lineages (Pardo-Manuel de Villena and Sapienza 2001, Blackmon et al. 2019), including fishes (Yoshida and Kitano 2012, Molina et al. 2014), particularly by a nonrandom segregation of rearranged chromosome in female meiosis of heterokaryotypes, due to inherent asymmetry of female meiosis and polarity of a meiotic spindle. Stronger spindles should bind bigger centromeres (Chmátal et al. 2014, Akera et al. 2019, Kursel and Malik 2018, Kumon and Lampson 2022). Yet the direction of the nonrandom segregation is not set in stone. Reversals of spindle polarity supposedly occurred in many phylogenetic groups, which could explain differences in trends in karyotype evolution between related taxa (Pardo-Manuel de Villena and Sapienza 2001, Yoshida and Kitano 2012, Blackmon et al. 2019). It is tempting to speculate that in *N. furzeri* and *N. kadleci*, the egg has a stronger spindle pole than in the other species under study, as they have considerably larger (peri)centromeric heterochromatin blocks comprising Nfu-SatA and Nfu-SatB in all chromosomes but the Y chromosome. Interestingly, in both *N. furzeri* and *N. kadleci* the large blocks of (peri)centric heterochromatin coincide with higher numbers of chromosome arms, but not with different number of chromosomes than expected when compared to karyotypes of other *Nothobranchius* spp. (Krysanov and Demidova 2018). It suggests that evolution of satellite DNA in *Nothobranchius* species is associated either with intrachromosomal rearrangements or centromere repositioning, i.e. inactivation of an existing centromere and de novo formation of a new one elsewhere on the chromosome (cf. Amor et al. 2004, Cappelletti et al. 2022).

To conclude, our cytogenetic and bioinformatic data suggests that centromere drive operates in *Nothobranchius* killifishes and shape their karyotypes. Reversal of spindle polarity probably occurred in the Southern clade and changed direction of the drive. Further research is needed to parse causes and consequences of karyotype evolution in the killifishes.

Acknowledgements: We would like to thank B. Nagy, A. Nikiforov and H. Hengstler for providing part of the study material and A. Nikiforov for his help in breeding and keeping fishes. We are also grateful to P. Šejnohová for the laboratory assistance.

Funding: This study was supported by The Czech Science Foundation (grant no. 19-22346Y (JŠ, PN, KL, AV, TP, MA, ŠP, MJ, AS) and further by RVO:67985904 of IAPG CAS, Liběchov (Czech Academy of Sciences) (MA, ŠP, AS) and the Charles University Research Centre program No. 204069 (MA). Computational resources were supplied by the project "e-Infrastruktura CZ" (e-INFRA LM2018140) provided within the program Projects of Large Research, Development and Innovations Infrastructures and the ELIXIR-CZ project (LM2018131), part of the international ELIXIR infrastructure. The funders had no role in study design, data collection and analysis, decision to publish, or preparation of the manuscript.

Conflicts of interest/Competing interests: The authors declare that they have no conflict of interest.

Availability of data and material: The following nucleotide sequences were deposited in NCBI GenBank: XXX. All other relevant data are within the paper and its Supporting Information file.

Authors' contributions: Conceptualization: AS, PN; Data curation: PN, AV, PM, MA; Formal analysis: PN, AV; Funding acquisition: AS; Investigation: AV, KL, PM, TP, MA, JŠ, ŠP, SAS, MJ, PN, AS; Methodology: AS, PN, AV, PM; Project administration: AS, PN; Resources: AS, PN, MR; Supervision: AS, PN, MR; Validation: AV, PM, AS, PN, MA; Writing original draft: AV, AS, PN, PM; Writing—review & editing: PN, AS, AV, PM, MA, JŠ, MR, SAS, CE.

Ethics approval: To prevent fish suffering, all handling of fish individuals followed European standards in agreement with §17 of the Act No. 246/1992 Coll. The procedures involving fishes were supervised by the Institutional Animal Care and Use Committee of the Institute of Animal Physiology and Genetics CAS, v.v.i., and the supervisor's permit number CZ 02361 was certified and issued by the Ministry of Agriculture of the Czech Republic. The experiments with *N. foerschi* and *N. cardinalis* were approved by the Ethics Committee of Severtsov Institute of Ecology and Evolution (Order No. 27 of November 9, 2018). For direct preparations of chromosomes from the kidney, fishes were euthanized using 2-phenoxyethanol (Sigma-Aldrich) before organ sampling. Fin samples (a narrow strip of the caudal fin) were taken from live individuals after fishes were anesthetized using MS-222 (Merck KGaA, Darmstadt, Germany).

Consent to participate: Not applicable

Consent for publication: Not applicable

6. References

Akera T, Trimm E, Lampson MA (2019) Molecular strategies of meiotic cheating by selfish centromeres. Cell 178:1132–1144. https://doi.org/10.1016/j.cell.2019.07.001

Amor DJ, Bentley K, Ryan J, Perry J, Wong L, Slater H, Choo KA (2004) Human centromere repositioning "in progress". Proc Natl Acad Sci USA 101:6542–6547. https://doi.org/10.1073/pnas.030863710

Andrews S (2010) FastQC: a quality control tool for high throughput sequence data [Online]. http://www.bioinformatics.babraham.ac.uk/projects/fastqc/

Ávila Robledillo L, Neumann P, Koblížková A, Novák P, Vrbová I, Macas J (2020) Extraordinary sequence diversity and promiscuity of centromeric satellites in the legume tribe Fabeae. Mol Biol Evol 37:2341–2356. https://doi.org/10.1093/molbev/msaa090

Bartáková V, Reichard M, Blažek R, Polačik M, Bryja J (2015) Terrestrial fishes: rivers are barriers to gene flow in annual fishes from the African savanna. J Biogeogr 42:1832–1844. https://doi.org/10.1111/jbi.12567

Berois N, García G, de Sá, RO, editors. Annual fishes: life history strategy, diversity and evolution. Boca Raton, FL: CRC Press; 2016.

Blackmon H, Justison J, Mayrose I, Goldberg EE (2019) Meiotic drive shapes rates of karyotype evolution in mammals. Evolution 73:511–523. https://doi.org/10.1111/evo.13682

Blažek R, Polačik M, Kačer P, Cellerino A, Řežucha R, Methling C, Tomášek O, Syslová K, Terzibasi Tozzini E, Albrecht T et al (2017) Repeated intraspecific divergence in life span and aging of African annual fishes along an aridity gradient. Evolution 71:386–402. https://doi.org/10.1111/evo.13127

Blažek R, Polačik M, Reichard M (2013) Rapid growth, early maturation and short generation time in African annual fishes. Evodevo 4:1–7. https://doi.org/10.1186/2041-9139-4-24

Bertollo LAC, Cioffi MB, Moreira-Filho O (2015) Direct chromosome preparation from freshwater teleost fishes. In: Ozouf-Costaz C, Pisano E, Foresti F, and de Almeida-Toledo LF (eds) Fish cytogenetic techniques: ray-fin fishes and chondrichthyans. CRC Press, Inc, Endfield, pp 21–26. https://doi. org/ 10. 1201/ b18534-4

Bracewell R, Chatla K, Nalley MJ, Bachtrog D (2019) Dynamic turnover of centromeres drives karyotype evolution in drosophila. Elife 8:1–47. https://doi.org/10.7554/eLife.49002

Cappelletti E, Piras FM, Sola L, Santagostino M, Abdelgadir WA, Raimondi E, Lescai F, Nergadze SG, Giulotto E (2022) Robertsonian fusion and centromere repositioning contributed to the formation of satellite-free centromeres during the evolution of zebras. Mol Biol Evol 39:1–21. https://doi.org/10.1093/molbev/msac162

Cech JN, Peichel CL (2016) Centromere inactivation on a neo-Y fusion chromosome in threespine stickleback fish. Chromosome Res 24:437–450. https://doi.org/10.1007/s10577-016-9535-7

Cellerino A, Valenzano DR, Reichard M (2016) From the bush to the bench: the annual *Nothobranchius* fishes as a new model system in biology. Biol Rev 91:511–533. https://doi.org/10.1111/brv.12183

Chang SB, Yang TJ, Datema E, Van Vugt J, Vosman B, Kuipers A, Meznikova M, Szinay D, Klein Lankhorst R, Jacobsen E, de Jong H (2008) FISH mapping and molecular organization of the major repetitive sequences of tomato. Chromosome Res 16:919–933. https://doi.org/10.1007/s10577-008-1249-z

Chaves R, Adega F, Heslop-Harrison JS, Guedes-Pinto H, Wienberg J (2003). Complex satellite DNA reshuffling in the polymorphic t (1; 29) Robertsonian translocation and evolutionarily derived chromosomes in cattle. Chromosome Res 11:641–648. https://doi.org/10.1023/A:1025952507959

Chmátal L, Gabriel SI, Mitsainas GP, Martínez-Vargas J, Ventura J, Searle JB, Schultz RM, Lampson MA (2014) Centromere strength provides the cell biological basis for meiotic drive and karyotype evolution in mice. Curr Biol 24:2295–2300. https://doi.org/10.1016/j.cub.2014.08.017

Conte MA, Joshi R, Moore EC, Nandamuri SP, Gammerdinger WJ, Roberts RB, Carleton KL, Lien S, Kocher T (2019) Chromosome-scale assemblies reveal the structural evolution of African cichlid genomes. Gigascience 8:1–20. https://doi.org/10.1093/gigascience/giz030

Cuadrado Á, Jouve N (2010) Chromosomal detection of simple sequence repeats (SSRs) using nondenaturing FISH (ND-FISH). Chromosoma 119, 495–503. https://doi.org/10.1007/s00412-010-0273-x

Cui R, Medeiros T, Willemsen D, Iasi LNM, Collier GE, Graef M, Reichard M, Valenzano DR (2019) Relaxed selection limits lifespan by increasing mutation load. Cell 178:385–399.e20. https://doi.org/10.1016/j.cell.2019.06.004

Ewulonu UK, Haas R, Turner B (1985) A multiple sex chromosome system in the annual killfish, *Nothobranchius guentheri*. Copeia 2:503–508. https://doi.org/10.2307/1444868

Ferreira IA, Poletto AB, Kocher TD, Mota-Velasco JC, Penman DJ, Martins C (2010) Chromosome evolution in african cichlid fish: Contributions from the physical mapping of repeated DNAs. Cytogenet Genome Res 129:314–322. https://doi.org/10.1159/000315895

Fricke R, Eschmeyer WN, Van der Laan R (eds) (2022) Eschmeyer's catalog of fishes: genera, species, references. http:// resea rchar chive. calac ademy. org/ resea rch/ ichth yology/ catal og/ fishc atmain. asp. Accessed 10 January 2023

Fry K, Salser W (1977) Nucleotide sequences of HS-α satellite DNA from kangaroo rat *Dipodomys ordii* and characterization of similar sequences in other rodents. Cell 12:1069–1084. https://doi.org/10.1016/0092-8674(77)90170-2

Furness AI (2016) The evolution of an annual life cycle in killifish: adaptation to ephemeral aquatic environments through embryonic diapause. Biol Rev Camb Philos Soc 91:796–812. https://doi.org/10.1111/brv.12194

Gamba R, Fachinetti D (2020) From evolution to function: two sides of the same CENP-B coin?. Exp Cell Res 390:111959. https://doi.org/10.1016/j.yexcr.2020.111959

Garrido-Ramos MA (2017) Satellite DNA: An evolving topic. Genes 8:230. https://doi.org/10.3390/genes8090230

Goes CAG, dos Santos RZ, Aguiar WRC, Alves DCV, Silva DMZA. Foresti F, Oliveira C, Utsunomia R, Porto-Foresti F (2022) Revealing the satellite DNA history in *Psalidodon* and *Astyanax* characid fish by comparative satellitomics. Front Genet 13:884072. https://doi.org/10.3389/fgene.2022.884072

Goes CAG, dos Santos N, Rodrigues PHM, Stornioli JHF, da Silva AB, dos Santos RZ, Vidal JAD, Silva DMZA, Artoni RF, Foresti F (2023) The satellite DNA catalogues of two Serrasalmidae (Teleostei, Characiformes): conservation of general satDNA features over 30 million years. Genes, 14:91. https://doi.org/10.3390/genes14010091

Haaf T, Schmid M (1984) An early stage of ZZ/ZW sex chromosomes differentiation in *Poecilia sphenops* var. *melanistica* (Poeciliidae, Cyprinodontiformes). Chromosoma 89:37–41. https://doi.org/10.1007/BF00302348

Hartley G, O'Neill RJ (2019) Centromere repeats: hidden gems of the genome. Genes 10:223. https://doi.org/10.3390/genes10030223

Henikoff S, Ahmad K, Malik HS (2001) The centromere paradox: stable inheritance with rapidly evolving DNA. Science 293:1098–1102. https://doi.org/10.1126/science.1062939

Hu CK, Brunet A (2018) The African turquoise killifish: a research organism to study vertebrate aging and diapause. Aging Cell 17:1–15. https://doi.org/10.1111/acel.12757

Ichikawa K, Tomioka S, Suzuki Y, Nakamura R, Doi K, Yoshimura J, Kumagai M, Inoue Y, Uchida Y, Irie N, Takeda H, Morishita S (2017) Centromere evolution and CpG methylation during vertebrate speciation. Nat Commun 8:1833. https://doi.org/10.1038/s41467-017-01982-7

Kim NS, Armstrong KC, Fedak G, Ho K, Park NI (2002) A microsatellite sequence from the rice blast fungus (Magnaporthe grisea) distinguishes between the centromeres of *Hordeum vulgare* and *H. bulbosum* in hybrid plants. Genome 45:165–174. https://doi.org/10.1139/G01-129

Kligerman AD, Bloom SE (1977) Rapid chromosome preparations from solid tissues of fishes. J Fish Res Board Can 34:266–269. https://doi.org/10.1139/f77-039

Kretschmer R, Goes CAG, Bertollo LAC, Ezaz T, Porto-Foresti F, Toma GA, Utsunomia R, Cioffi MB (2022) Satellitome analysis illuminates the evolution of ZW sex chromosomes of Triportheidae fishes (Teleostei: Characiformes). Chromosoma. https://doi.org/10.1007/s00412-022-00768-1

692 Krysanov E, Demidova T, Nagy B (2016) Divergent karyotypes of the annual killifish genus
693 *Nothobranchius* (Cyprinodontiformes, Nothobranchiidae). Comp Cytogenet 10:439–445.
694 https://doi.org/10.3897/CompCytogen.v10i3.9863

695 Krysanov E, Demidova T (2018) Extensive karyotype variability of African fish genus
696 Nothobranchius (Cyprinodontiformes). Comp Cytogenet 12:387–402.
697 https://doi.org/10.3897/CompCytogen.v12i3.25092

698 Krysanov EY, Nagy B, Watters BR, Sember A, Simanovsky SA (2023) Karyotype
699 differentiation in the *Nothobranchius ugandensis* species group (Teleostei,
700 Cyprinodontiformes), seasonal fishes from the east African inland plateau, in the context of
701 phylogeny and biogeography. Comp Cytogenet 7:13–29.
702 https://doi.org/10.3897/compcytogen.v7.i1.97165

703 Kumon T, Lampson MA (2022) Evolution of eukaryotic centromeres by drive and suppression
704 of selfish genetic elements. Semin Cell Dev Biol.
705 https://doi.org/10.1016/j.semcdb.2022.03.026

706 Kursel LE, Malik HS (2018) The cellular mechanisms and consequences of centromere drive.
707 Curr Opin Cell Biol 52:58–65. https://doi.org/10.1016/j.ceb.2018.01.011

708 Levan AK, Fredga K, Sandberg AA (1964) Nomenclature for centromeric position on
709 chromosomes. Hereditas 52:201– 220. https://doi.org/10.1111/j.1601-5223.1964.tb01953.x

710 Mayr B, Ráb P, Kalat M (1985) Localisation of NORs and counterstain-enhanced fluorescence
711 studies in *Perca fluviatilis* (Pisces, Percidae). Genetica 67:51–56.
712 https://doi.org/10.1007/BF02424460

713 Martin M (2011) Cutadapt removes adapter sequences from high-throughput sequencing
714 reads. EMBnet.journal 17:10–12. https://doi.org/10.14806/ej.17.1.200

715 McKinley KL, Cheeseman IM (2016). The molecular basis for centromere identity and
716 function. Nat Rev Mol Cell Biol, 17:16–29. https://doi.org/10.1038/nrm.2015.5

717 Melters DP, Bradnam KR, Young HA, Young HA, Telis N, May MR, Ruby JG, Sebra R, Peluso
718 P, Eid J, Rank D et al (2013) Comparative analysis of tandem repeats from hundreds of
719 species reveals unique insights into centromere evolution. Genome Biol 14:R10.
720 https://doi.org/10.1186/gb-2013-14-1-r10

721 Molina WF, Martinez P a., Bertollo LAC, Bidau CJ (2014) Evidence for meiotic drive as an
722 explanation for karyotype changes in fishes. Mar Genomics 15:29–34.
723 https://doi.org/10.1016/j.margen.2014.05.001

724 Nagy B (2018) *Nothobranchius ditte*, a new species of annual killifish from the Lake Mweru
725 basin in the Democratic Republic of the Congo (Teleostei: Nothobranchiidae). Ichthyol Explor
726 Freshw 28:115–134.

727 Nagy B, Watters BR (2021) A review of the conservation status of seasonal *Nothobranchius*
728 fishes (Teleostei: Cyprinodontiformes), a genus with a high level of threat, inhabiting
729 ephemeral wetland habitats in Africa. Aquat Conserv 32: 199–216.
730 https://doi.org/10.1002/aqc.3741

Nishihara H, Stanyon R, Tanabe H, Koga A (2021) Replacement of owl monkey centromere satellite by a newly evolved variant was a recent and rapid process. Genes Cells 26:979–986. https://doi.org/10.1111/gtc.12898

Novák P, Neumann P, Macas, J (2020) Global analysis of repetitive DNA from unassembled sequence reads using RepeatExplorer2. Nat Protoc 15, 3745–3776. https://doi.org/10.1038/s41596-020-0400-y

Pardo-Manuel De Villena F, Sapienza C (2001) Nonrandom segregation during meiosis: The unfairness of females. Mamm Genome 12:331–339. https://doi.org/10.1007/s003350040003

Plohl M, Meštrović N, Mravinac B (2012) Satellite DNA evolution. Genome Dyn 7:126–152. https://doi.org/10.1159/000337122

Pokorná M, Altmanová M, Kratochvíl L (2014) Multiple sex chromosomes in the light of female meiotic drive in amniote vertebrates. Chromosome Res 22:35–44. https://doi.org/10.1007/s10577-014-9403-2

Ráb P, Roth P (1988) Cold-blooded vertebrates. In: Balicek P, Forejt J, Rubeš J (eds) Methods of chromosome analysis. Cytogenetická Sekce Československé Biologické Společnosti při CSAV, Brno, Czech Republic, pp 115–124

Reichard M, Giannetti K, Ferreira T, Maouche A, Vrtílek M, Polačik M, Blažek R, Ferreira MG (2022) Lifespan and telomere length variation across populations of wild-derived African killifish. Mol Ecol 31:5979–5992. https://doi.org/10.1111/mec.16287

Reichwald K, Lauber C, Nanda I, Kirschner J, Hartmann N, Schories S, Gausmann U, Taudien S, Schilhabel MB, Szafranski K et al (2009) High tandem repeat content in the genome of the short-lived annual fish *Nothobranchius furzeri*: a new vertebrate model for aging research. Genome Biol 10:R16. https://doi.org/10.1186/gb-2009-10-2-r16

Reichwald K, Petzold A, Koch P, Downie BR, Hartmann N, Pietsch S, Baumgart M, Chalopin D, Felder M, Bens M et al (2015) Insights into sex chromosome evolution and aging from the genome of a short-lived fish. Cell 163:1527–1538. https://doi.org/10.1016/j.cell.2015.10.071

Ruiz-Ruano FJ, López-León MD, Cabrero J, Camacho JPM (2016) High-throughput analysis of the satellitome illuminates satellite DNA evolution. Sci Rep 6:28333. https://doi.org/10.1038/srep28333

Sember A, Bohlen J, Šlechtová V, Altmanová M, Symonová R, Ráb P (2015) Karyotype differentiation in 19 species of river loach fishes (Nemacheilidae, Teleostei): extensive variability associated with rDNA and heterochromatin distribution and its phylogenetic and ecological interpretation. BMC Evol Biol 15:251. https://doi.org/10.1186/s12862-015-0532-9

Sola L, Rossi AR, Iaselli V, Rasch EM, Monaco PJ (1992) Cytogenetics of bisexual/unisexual species of *Poecilia*. II. Analysis of heterochromatin and nucleolar organizer regions in *Poecilia mexicana mexicana* by C-banding and DAPI, quinacrine, chromomycin A_3, and silver staining. Cytogenet Cell Genet 60:229–235. https://doi. org/10.1159/000133346

Stornioli JHF, Goes CAG, Calegari RM, dos Santos RZ, Giglio LM, Foresti F, Oliveira C, Penitente M, Porto-Foresti F, Utsunomia R (2021). The B chromosomes of *Prochilodus lineatus* (Teleostei, Characiformes) are highly enriched in satellite DNAs. Cells 10:1527. https://doi.org/10.3390/cells10061527

772 Štundlová, J, Hospodářská M, Lukšíková K, Voleníková A, Pavlica T, Altmanová M, Richter A,
773 Reichard M, Dalíková M, Pelikánová Š, Marta, A, Simanovsky SA, Hiřman M, Jankásek M,
774 Dvořák T, Bohlen J, Ráb P, Englert C, Nguyen P, Sember A (2022) Sex chromosome
775 differentiation via changes in the Y chromosome repeat landscape in African annual killifishes
776 *Nothobranchius furzeri* and *N. kadleci*. Chromosome Res 30:309–33.
777 https://doi.org/10.1007/s10577-022-09707-3

778 Suntronpong A, Kugou K, Masumoto H, Srikulnath K, Ohshima K, Hirai H, Koga A (2016)
779 CENP-B box, a nucleotide motif involved in centromere formation, occurs in a New World
780 monkey. Biol Lett 12:20150817. https://doi.org/10.1098/rsbl.2015.0817

781 Suntronpong A, Singchat W, Kruasuwana W, Prakhongcheep O, Sillapaprayoon S, Muangmai
782 N, Somyong S, Indananda C, Kraichak E, Peyachoknagul S, Srikulnath K (2020)
783 Characterization of centromeric satellite DNAs (MALREP) in the Asian swamp eel (*Monopterus*
784 *albus*) suggests the possible origin of repeats from transposable elements. Genomics
785 112:3097–3107. https://doi.org/10.1016/j.ygeno.2020.05.024

786 Talbert PB, Henikoff S (2020) What makes a centromere? Exp Cell Res 389:111895.
787 https://doi.org/10.1016/j.yexcr.2020.111895

788 Tao W, Xu L, Zhao L, Zhu Z, Wu X, Min Q, Wang D, Zhou Q (2021) High-quality chromosome-
789 level genomes of two tilapia species reveal their evolution of repeat sequences and sex
790 chromosomes. Mol Ecol Resour 21:543–560. https://doi.org/10.1111/1755-0998.13273

791 Terzibasi Tozzini E, Cellerino A (2020) *Nothobranchius* annual killifishes. Evodevo 11:25.
792 https://doi.org/10.1186/s13227-020-00170-x

793 Thakur J, Packiaraj J, Henikoff S (2021) Sequence, chromatin and evolution of satellite DNA.
794 Int J Mol Sci 22:4309. https://doi.org/10.3390/ijms22094309

795 The Galaxy Community (2022) The Galaxy platform for accessible, reproducible and
796 collaborative biomedical analyses: 2022 update. Nucleic Acids Research 50: W345–W351.
797 https://doi.org/10.1093/nar/gkac247

798 van der Merwe PDW, Cotterill FPD, Kandziora M, Watters BR, Nagy B, Genade T, Flügel TJ,
799 Svendsen DS, Bellstedt DU (2021) Genomic fingerprints of palaeogeographic history: the
800 tempo and mode of rift tectonics across tropical Africa has shaped the diversification of the
801 killifish genus *Nothobranchius* (Teleostei: Cyprinodontiformes). Mol Phylogenet Evol
802 158:106988. https://doi.org/10.1016/j.ympev.2020.106988

803 Varadharajan S, Rastas P, Löytynoja A, Matschiner M, Calboli FCF, Guo B, Nederbragt AJ,
804 Jakobsen KS, Merilä J (2019) A high-quality assembly of the nine-spined stickleback
805 (*Pungitius pungitius*) genome. Genome Biol Evol 11:3291–3308.
806 https://doi.org/10.1093/gbe/evz240

807 Völker M, Ráb P (2015) Direct chromosome preparation from regenerating fin tissue. In: Ozouf-
808 Costaz C, Pisano E, Foresti F, and de Almeida-Toledo LF (eds) Fish cytogenetic techniques:
809 ray-fin fishes and chondrichthyans. CRC Press, Inc, Endfield, pp 37–41.
810 https://doi.org/10.1201/b18534-4

811 Watters BR, Cooper BJ, Wildekamp RH (2008) Description of *Nothobranchius cardinalis*
812 spec. nov. (Cyprinodontiformes: Aplocheilidae), an annual fish from the Mbwemkuru River
813 basin, Tanzania. J. Am. Killifsh Ass. 40(5&6):129–145.

814 Watters BR, Nagy B, van der Merwe PDW, Cotterill FPD, Bellstedt DU (2020) Redescription
815 of the seasonal killifish species *Nothobranchius ocellatus* and description of a related new
816 species *Nothobranchius matanduensis*, from eastern Tanzania (Teleostei: Nothobranchiidae).
817 Ichthyol Explor Freshw 30:151–178. http://doi.org/10.23788/IEF-1149

818 Wildekamp RH (1996) A world of killies. Atlas of the oviparous cyprinodontiform fishes of the
819 world (Vol. III). American Killifish Association, Mishawaka, 330 pp.

820 Wildekamp RH (2004) A world of killies – atlas of the oviparous cyprinodontiform fishes of the
821 world (Vol. 4). The American Killifish Association, Elyria, Ohio

822 Willemsen D, Cui R, Reichard M, Valenzano DR (2020) Intra-species differences in population
823 size shape life history and genome evolution. Elife 9:e55794.
824 https://doi.org/10.7554/eLife.55794

825 Yano CF, Bertollo LAC, Ezaz T, Trifonov V, Sember A, Liehr T, Cioffi MB (2017) Highly
826 conserved Z and molecularly diverged W chromosomes in the fish genus *Triportheus*
827 (Characiformes, Triportheidae). Heredity 118:276–283. https://doi.org/10.1038/ hdy.2016.83F

828 Yoshida K, Kitano J (2012) The contribution of female meiotic drive to the evolution of neo-sex
829 chromosomes. Evolution 66:3198–3208. https://doi.org/10.1111/j.1558-5646.2012.01681.x

830

831
832
833
834
835
836
837
838
839
840
841
842
843
844
845
846
847
848
849
850
851
852

7. Supplementary material

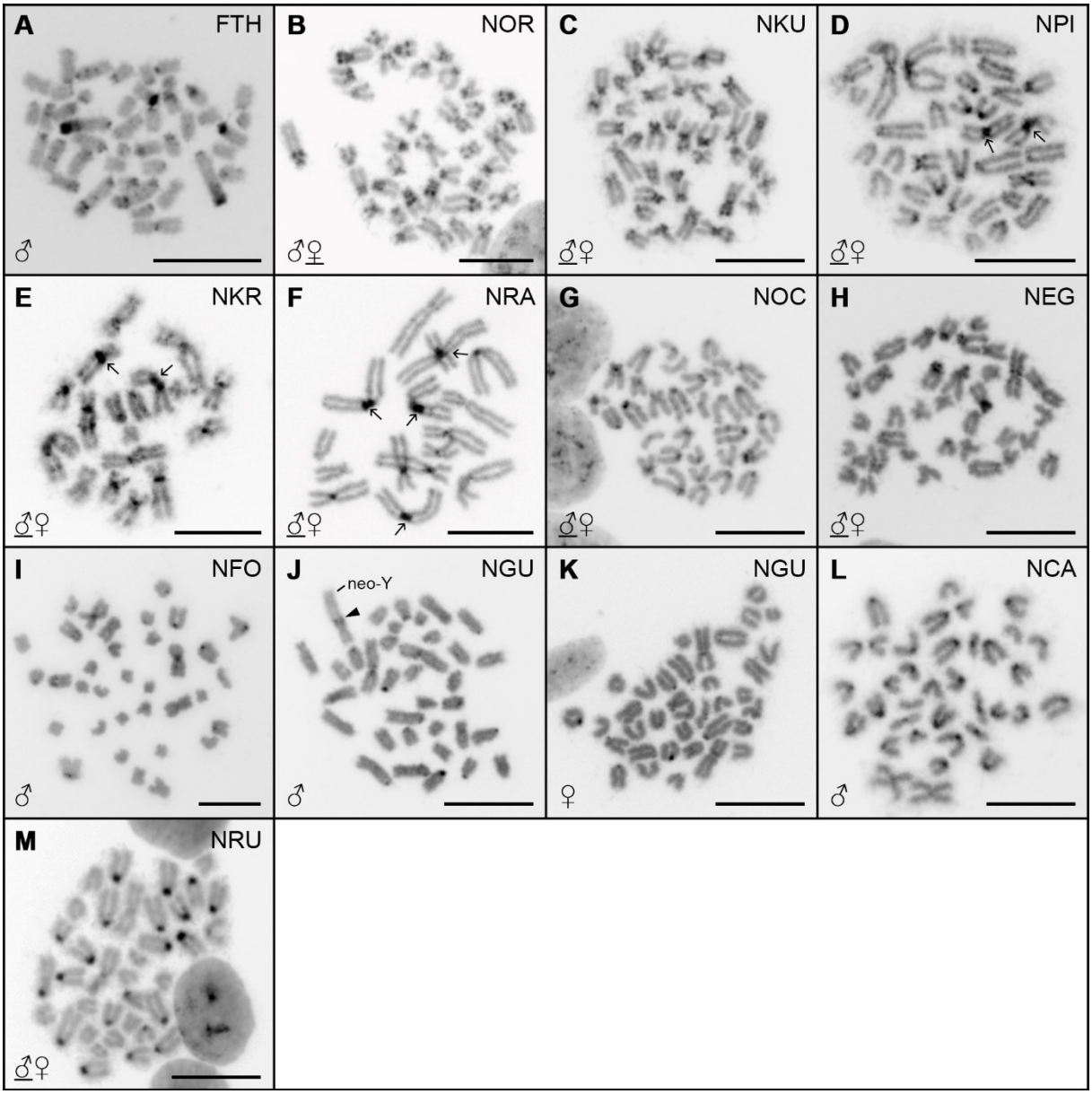

Supplementary Fig. 1 Mitotic metaphases of *F. thierryi* and *Nothobranchius* spp. after C-banding. Sex of the studied individuals is indicated and eventually underlined where both sexes (if studied) presented the same distribution pattern (i.e. except for *N. guentheri*; J, K). Arrows indicate examples of huge (peri)centromeric heterochromatin blocks in expected fusion sites on large metacentric chromosomes in the Southern-clade species (D–F). Neo-Y chromosome in *N. guentheri* male (J) is identified based on its distinctive morphology; full arrowhead points to the heterochromatin block representing an assumed fusion site. Chromosomes stained with DAPI (inverted colors). Scale bar = 10 μm

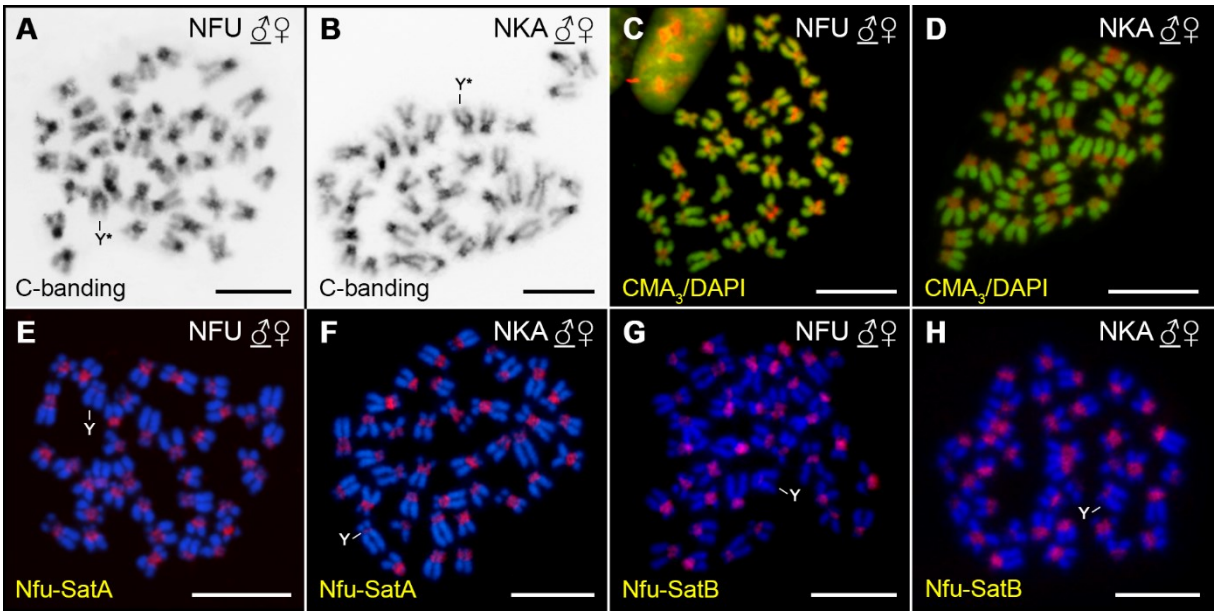

Supplementary Fig. 2 Mitotic metaphases of *N. furzeri* and *N. kadleci* after various cytogenetic treatments. (A, B) C-banding, (C, D), CMA_3/DAPI staining, (E, F) FISH with Nfu-SatA probe, (G, H), FISH with Nfu-SatB probe. All metaphases are adopted from the Supplementary material of our previous work (Štundlová et al. 2022) and serve here as a direct comparison of patterns revealed in the present study. The presented metaphases belong to male representatives of the same populations as used in the present study: *N. furzeri* MZCS-222 and *N. kadleci* MZCS-91. Assumed Y sex chromosomes are marked if detectable. Chromosomes were counterstained with DAPI (blue). Images follow the same color coding as the remaining supplementary figs in the present study (depending on the method used). Scale bar = 10 μ

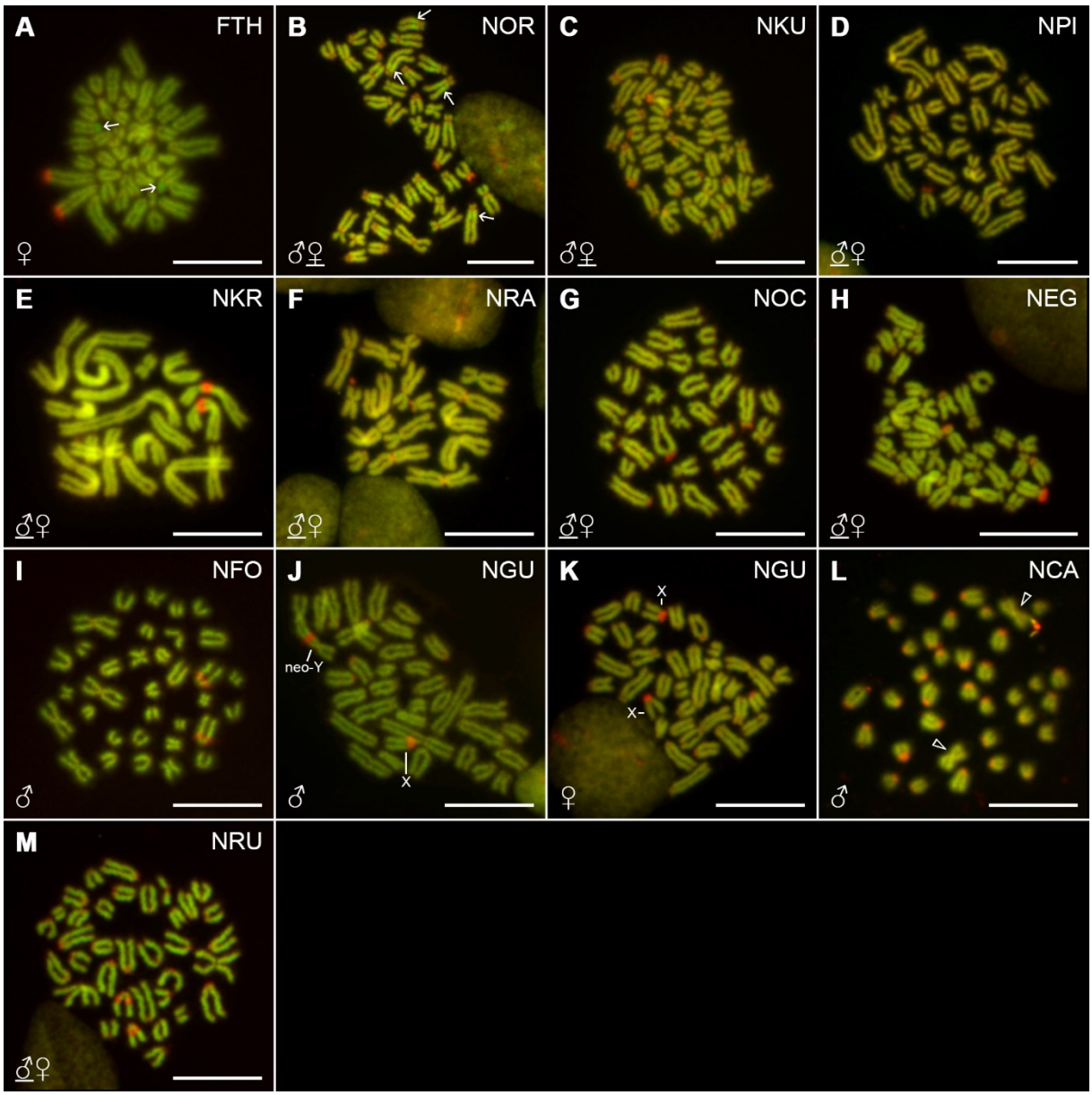

Supplementary Fig. 3 Mitotic metaphases of *F. thierryi* and *Nothobranchius* spp. after CMA_3/DAPI staining. Sex of the studied individuals is indicated and eventually underlined where both sexes (if studied) presented the same distribution pattern (i.e. except for *N. guentheri*; J, K). For better contrast, images were pseudocolored in red (for CMA_3) and green (for DAPI). Neo-Y chromosome and one of the X chromosomes in *N. guentheri* male (J) are identified based on distinctive morphology and shared strong CMA_3^+ signals, respectively. Both X homologs are marked in *N. guentheri* female (K). In *N. cardinalis* (L) empty arrowheads point to the only metacentric chromosomes in the complement which are also the only elements lacking the (peri)centromeric CMA_3 signals. Arrows point to examples of rarely observed pronounced AT-rich regions (A, B). Scale bar = 10 μm

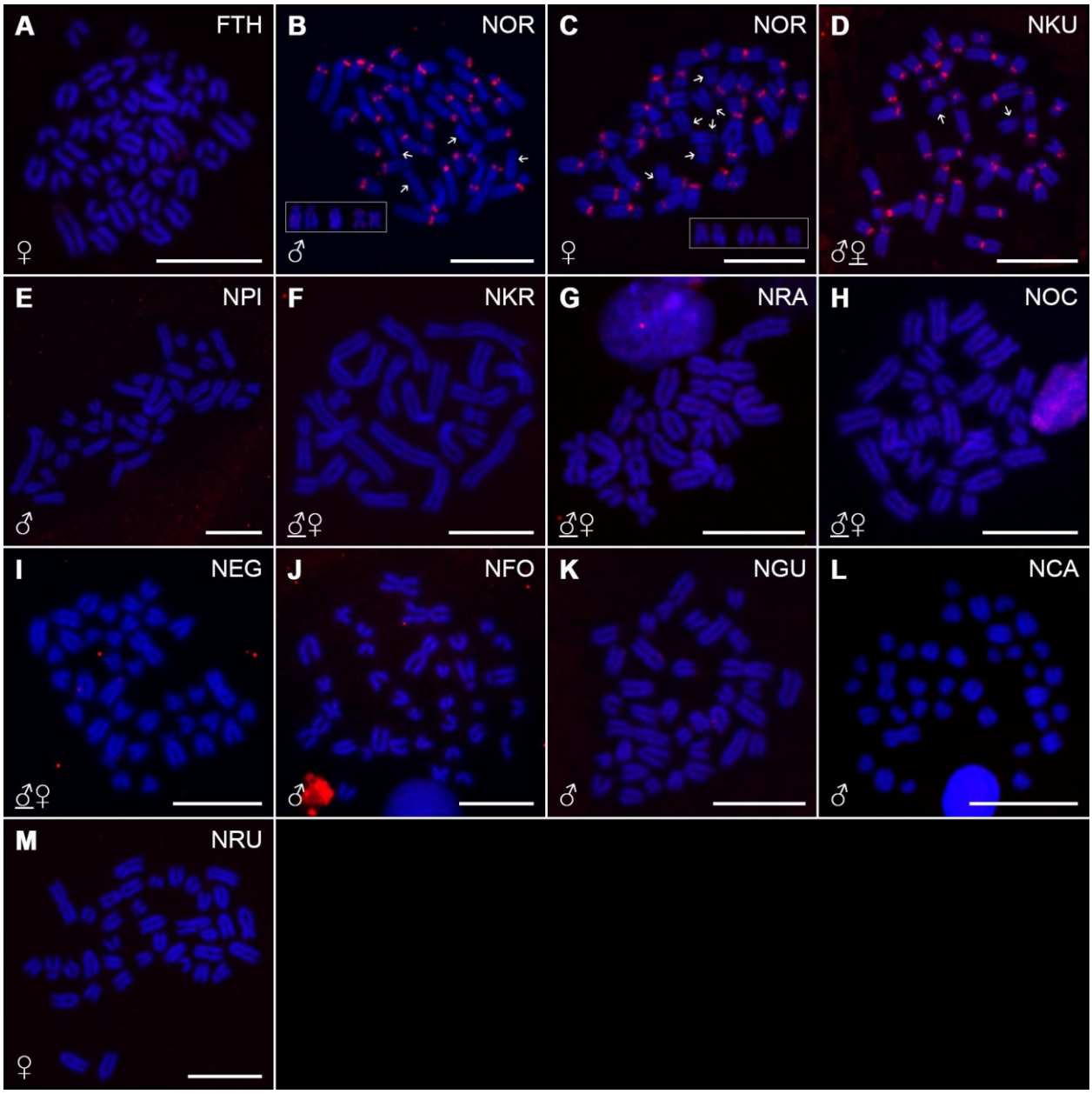

Supplementary Fig. 4 Mitotic metaphases of *F. thierryi* and *Nothobranchius* spp. after FISH with Nfu-SatA repeat (red signals). Sex of the studied individuals is indicated and eventually underlined where both sexes (if studied) presented the same distribution pattern (i.e. except for *N. orthonotus*; B, C). In *N. orthonotus* (B, C), arrows point to chromosomes lacking the (peri)centromeric signals. Polymorphic patterns regarding this feature are framed. Chromosomes were counterstained with DAPI (blue). Scale bar = 10 µm

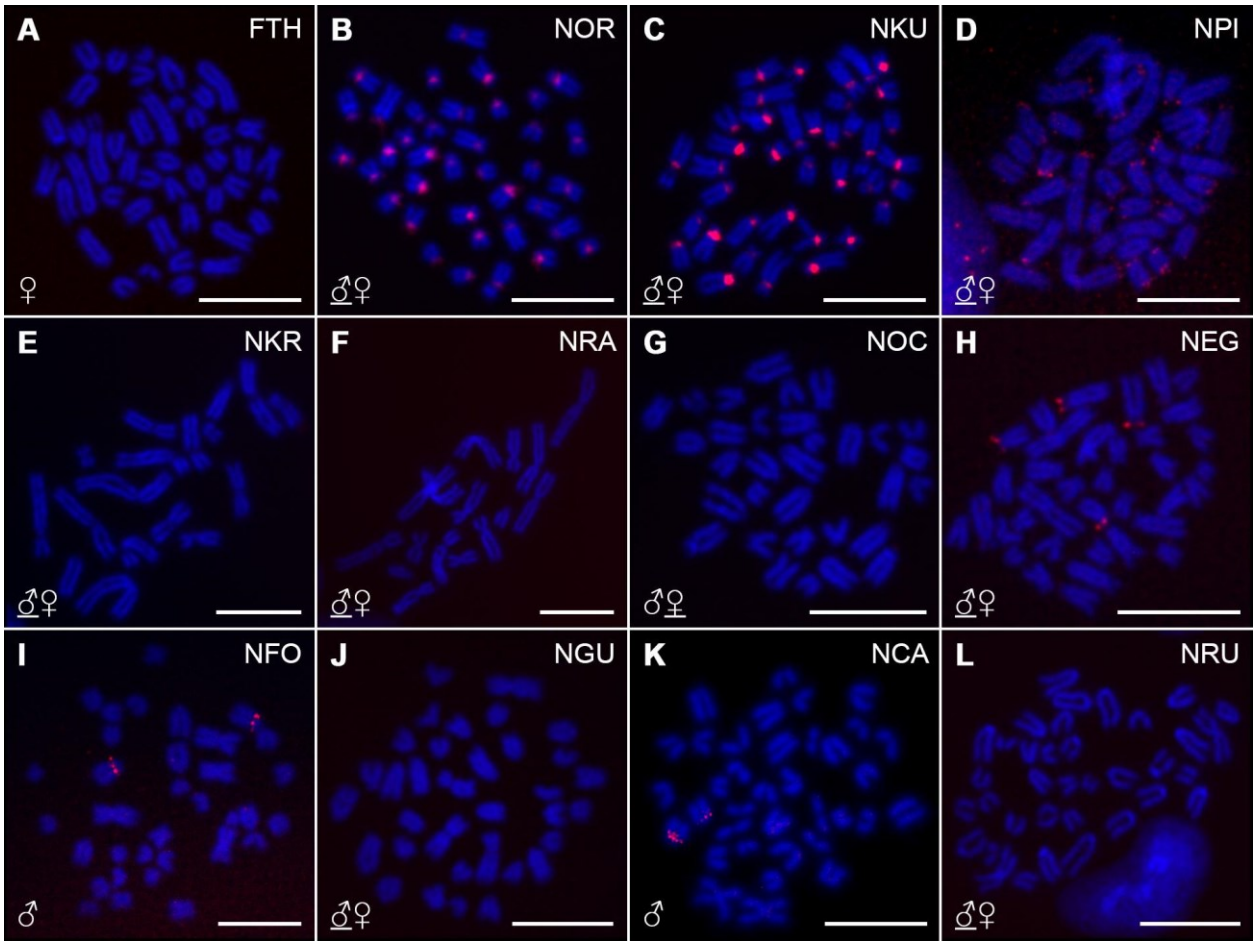

Supplementary Fig. 5 Mitotic metaphases of *F. thierryi* and *Nothobranchius* spp. after FISH with Nfu-SatB repeat (red signals). Sex of the studied individuals is indicated and eventually underlined where both sexes (if studied) presented the same distribution pattern. Chromosomes were counterstained with DAPI (blue). Scale bar = 10 μm

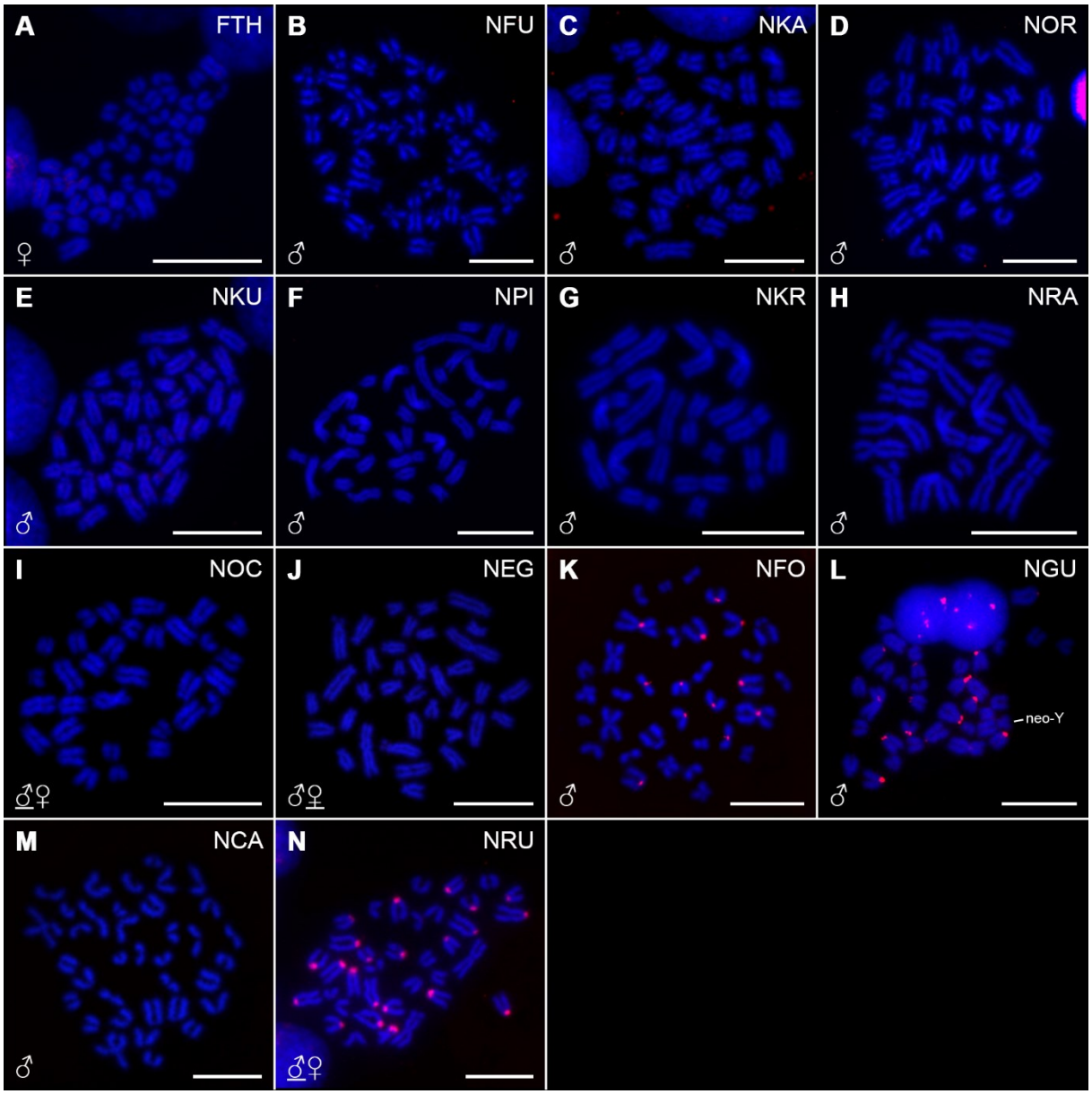

Supplementary Fig. 6 Mitotic metaphases of *F. thierryi* and *Nothobranchius* spp. after FISH with Cl-36 repeat (red signals). Sex of the studied individuals is indicated and eventually underlined where both sexes (if studied) presented the same distribution pattern. Neo-Y chromosome in *N. guentheri* male (L) is identified based on distinctive morphology. Chromosomes were counterstained with DAPI (blue). Scale bar = 10 μm

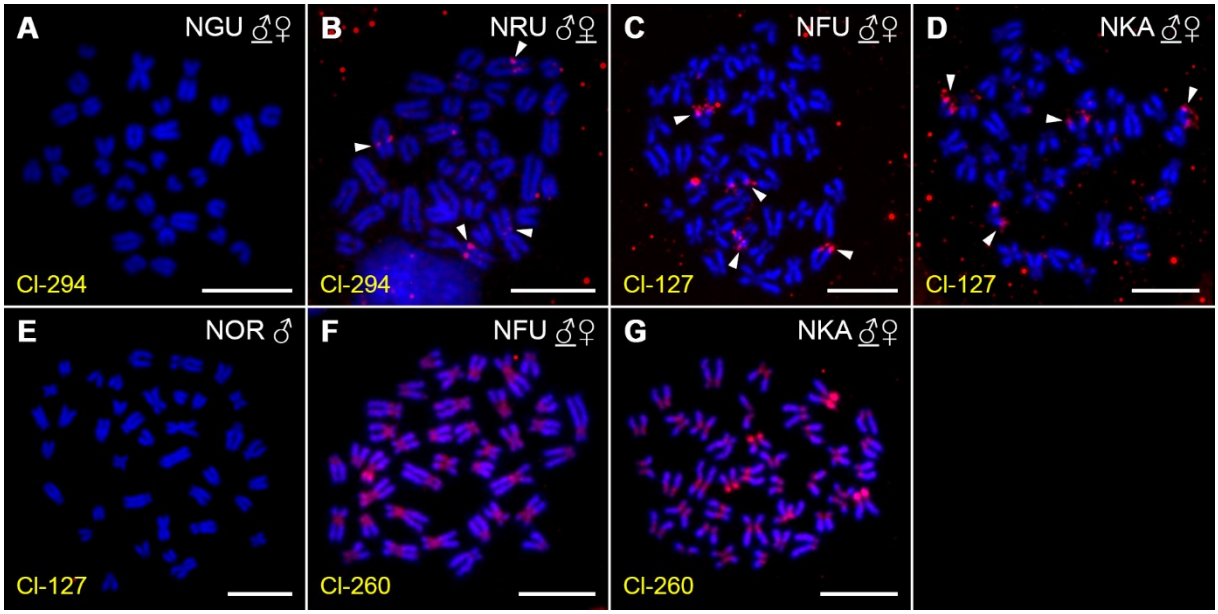

Supplementary Fig. 7 Mitotic metaphases of selected *Nothobranchius* spp. after FISH with three different satDNA probes (red signals and arrowheads in B–D). Sex of the studied individuals is indicated and eventually underlined where both sexes (if studied) presented the same distribution pattern. Chromosomes were counterstained with DAPI (blue). Scale bar = 10 μm

Supplementary Table 1. A detailed list of studied *Nothobranchius* killifish species with their sample sizes (N) used for each method, population/collection codes, source/geographic origin and GPS coordinates of sampling localities

Clade	Species	Code	*N*									Population (collection code)	Source / locality	GPS coordinates
			C-banding	CMA_3	Nfu-SatA	Nfu-SatB	CI-127	CI-260	CI-36	CI-294	Summary			
outgroup	*Fundulosoma thierryi* Ahl, 1924	FTH	1♂, 2♀	2♀	2♀	2♀	–	–	3♀	–	1♂, 3♀	aquarium strain	–	–
Southern clade	*Nothobranchius furzeri* Jubb, 1971	NFU	*	*	*	*	1♂, 1♀	1♂, 1♀	2♂	–	1♂, 1♀	MZCS-222	Chefu, Mozambique	21°52'24.8"S 32°48'2.3"E
	N. kadleci Reichard, 2010	NKA	*	*	*	*	1♂, 1♀	1♂, 1♀	1♂	–	1♂, 1♀	MZCS-91	Gorongosa, Mozambique	20°41'16.6"S 34°6'21.9"E
	N. orthonotus (Peters, 1844)	NOR	2♂, 3♀	1♂, 1♀	3♂, 3♀	1♂, 1♀	1♂, 2♀	–	1♂	–	3♂, 3♀	MZCS-02	Limpopo, Mozambique	24°03'48.5"S 32°43'55.9"E
	N. kuhntae (Ahl, 1926)	NKU	4♂, 1♀	1♂, 2♀	3♂, 3♀	1♂, 1♀	–	–	2♂	–	4♂, 3♀	MZCS-528	Pungwe, Mozambique	19°41'50.5"S 34°46'58.6"E
	N. pienaari Shidlovskyi, Watters & Wildekamp, 2010	NPI	2♂, 2♀	2♂, 3♀	2♂	2♂, 2♀	–	–	1♂	–	2♂, 3♀	MZCS-505	Limpopo, Mozambique	23°31'47.2"S 32°34'40.6"E
	N. krysanovi Shidlovskyi, Watters & Wildekamp, 2010	NKR	2♂, 2♀	1♂, 2♀	1♂, 2♀	1♂, 2♀	–	–	1♂	–	2♂, 2♀	aquarium strain; MZCS-249	Quelimane, Mozambique	17°48'52.2"S 36°54'49.4"E
	N. rachovii Ahl, 1926	NRA	2♂, 2♀	1♂, 1♀	1♂, 1♀	1♂, 1♀	–	–	1♂	–	2♂, 2♀	MZCS-096	Beira Airport, Mozambique	19°48'48.8"S 34°54'17.6"E
Ocellatus clade	*N. ocellatus* (Seegers, 1985)	NOC	1♂, 1♀	1♂, 1♀	1♂, 1♀	1♂, 1♀	–	–	1♂, 1♀	–	1♂, 1♀	population mix	Nyamwage, Tanzania	–
Coastal clade	*N. eggersi* Seegers, 1982	NEG	2♂, 1♀	1♂, 1♀	2♂, 1♀	1♂, 1♀	–	–	2♂, 1♀	–	2♂, 1♀	T52	Bagamoyo, Tanzania	6°28'55.9"S 38°54'51.5"E
	N. foerschi Wildekamp & Berkenkamp, 1979	NFO	2♂	2♂	2♂	2♂	–	–	2♂	–	2♂	CI 57	Soga, Tanzania	6°50'13.2"S 38°50'45.6"E
	N. guentheri (Pfeffer, 1983)	NGU	3♂, 3♀	4♂, 2♀	1♂, 2♀	1♂, 2♀	–	–	2♂	2♂, 1♀	4♂, 3♀	aquarium strain	Zanzibar, Tanzania	–
	N. cardinalis Watters, Cooper & Wildekamp, 2008	NCA	1♂	1♂	1♂	1♂	–	–	1♂	–	1♂	TTKSN 17-12	Matandu, Tanzania	9°30'04.0"S 38°13'49.0"E
	N. rubripinnis Seegers, 1986	NRU	1♂, 1♀	1♂, 2♀	2♀	2♂	–	–	2♂, 2♀	1♂, 2♀	2♂, 2♀	T33	Kitonga, Tanzania	7°12'40.5"S 39°10'30.9"E